Electronic Supplementary Material (ESI) for Chemical Communications

Supporting Information for

Facile preparation of chiral penicillamine protected gold nanoclusters and their applications in cell imaging

Xuan Yang, Linfeng Gan, Lei Han, Dan Li, Jin Wang* and Erkang Wang*

State Key Laboratory of Electroanalytical Chemistry, Changchun Institute of Applied Chemistry, Chinese Academy of Sciences, Changchun, Jilin,130022, China, Graduate School of the Chinese Academy of Sciences, Beijing, 100039, China, College of Physics, Jilin University, Changchun, Jilin, P. R. China 130012 and Department of Chemistry and Physics, State University of New York at Stony Brook, New York 11794-3400.

*To whom correspondence should be addressed. E-mail: jin.wang.1@stonybrook.edu; ekwang@ciac.jl.cn

Experiment Section:

Chemicals: Tetrakis(hydroxymethyl)phosphonium chloride (THPC, $P(CH_2OH)_4Cl$, 80% aqueous solution), L-penicillamine, D-penicillamine and DL-penicillamine were purchased from Acros Organics (Belgium). All the other chemicals were of analytical reagent grade and were used as received without further purification. All the solutions were prepared with double-distilled water purified by a Milli-Q system (Millipore, Bedford, MA, USA).

Synthesis of Au NCs: In a typical experiment, 12 μL THPC was added to 47 mL NaOH solution (6 mM) at 25 °C. The mixture was stirred for 3 min, followed by rapid addition of a solution of $HAuCl_4$ (0.67 mL, 2% by mass) and chiral PA (2.5 mL, 0.1 M). After stirring for about 15 h, the solution changed from colorless to light yellow. In a typical experiment, 12 μL THPC was added to 47 mL NaOH solution (6 mM) at 25 °C. The mixture was stirred for 3 min, followed by rapid addition of a solution of $HAuCl_4$ (0.67 mL, 2% by mass) and chiral PA (2.5 mL, 0.1 M). After stirring for about 15 h, the solution changed from colorless to light yellow.

Characterizations. UV-visible absorbance spectra were recorded on a Cary 50 scan UV-vis-NIR spectrophotometer (Varian, Harbor City, CA) at room temperature. Photoluminescence spectra were carried out on a LS-55 luminescence spectrometer (Perkin-Elmer). Mass spectrometry (MS) was carried out on Bruker autoflex III smartbeam MALDI-TOF/TOF-MS (Germany), the laser system was smartbeam laser with 355nm wavelegnth and the scan mode was reflective/linear, the ion mode was positive under an acceleration voltage of 20.00 kV, the ion extraction time was 0 ns, the solvent was water and the matrix was 2, 5-dihydroxylbezonic acid. TEM measurements and EDS were made on a FEI TECNAI G^2 transmission electron microscope (Netherlands) operated at an accelerating voltage of 120 kV. XPS measurements were made on a Thermo ESCALAB 250 X-ray photoelectron spectrometer. AFM measurement was carried out on a MultiMode® 8 Scanning Probe Microscope (Veeco Instruments Inc., USA) at room temperature, analyzed with NanoScope® Version 8.1 software. CD spectra were collected using a JASCO J-820 spectropolarimeter (Tokyo, Japan) and CD measurements were from 200 to 400 nm, the data pitch was 0.1 nm, scan speed was 200 nm/min, response time was 0.5 s, and bandwidth was 1 nm.

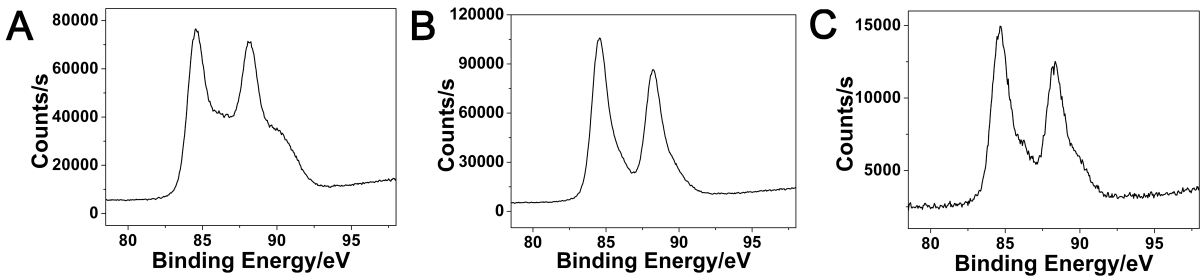

Figure S1. XPS spectra showing the binding energy of the Au4f level of L-Au NCs (A), D-Au NCs (B) and DL-Au NCs (C).

XPS measurements were carried out to analyze the valence states of gold in chiral PA protecctd Au NCs. As shown in Figure S1 A, the binding energy of $Au4f_{7/2}$ and $Au4f_{5/2}$ were at 84.5 eV and 88.1 eV, respectively. It was noteworthy that the binding energy of $Au4f_{7/2}$ fell between the Au (0) (84 eV) of a metallic gold film and the Au (I) (86 eV) of gold thiolate, which indicated the coexistence of Au (0) and Au (I) in L-Au NCs. Similar results were observed in D-Au NCs and DL-Au NCs as shown in Figure S1 B and Figure S1 C, respectively.

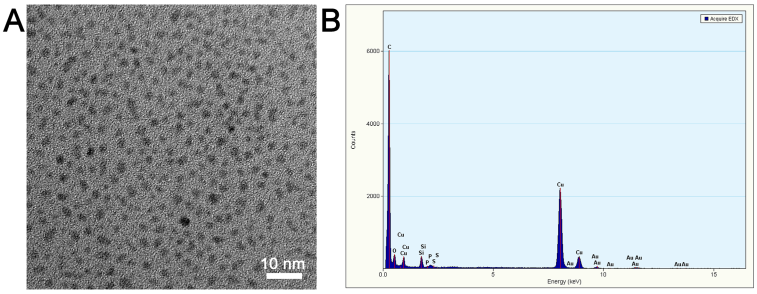

Figure S2. The TEM image and EDS spectrum of L-Au NCs.

As shown in Figure S2, the diameters of L-Au NCs were mostly smaller than 2 nm and such Au NCs were constructed with Au.

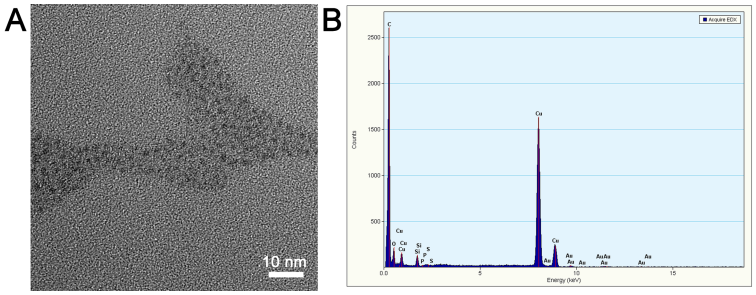

Figure S3. The TEM image and EDS spectrum of D-Au NCs.

As shown in Figure S3, the diameters of D-Au NCs were mostly smaller than 2 nm and such Au NCs were constructed with Au.

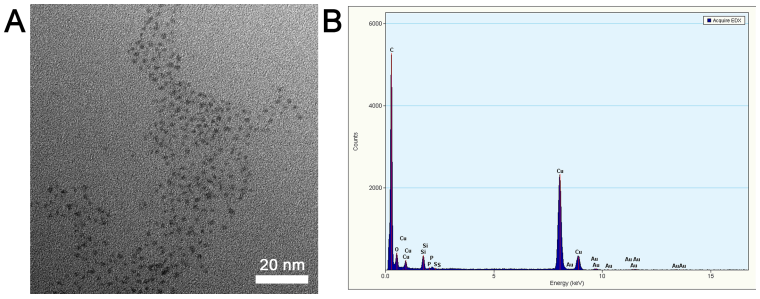

Figure S4. The TEM image and EDS spectrum of DL-Au NCs.

As shown in Figure S4, the diameters of DL-Au NCs were mostly smaller than 2 nm and such Au NCs were constructed with Au.

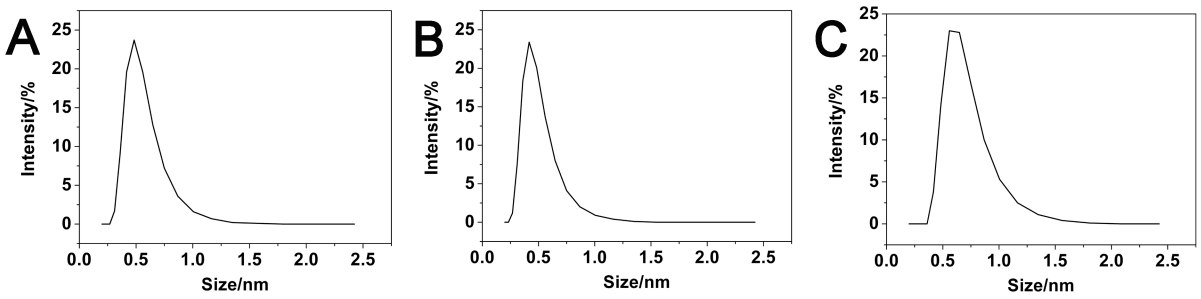

Figure S5. The dynamic light scattering results of chiral PA protected Au NCs, A: L-Au NCs, B: D-Au NCs, C: DL-Au NCs.

The dynamic light scattering results in Figure S5 showed that the diameters of chiral PA protected Au NCs were mostly about 0.5 nm which were consistent with the TEM images and AFM images in Figure 1 and Figure S6.

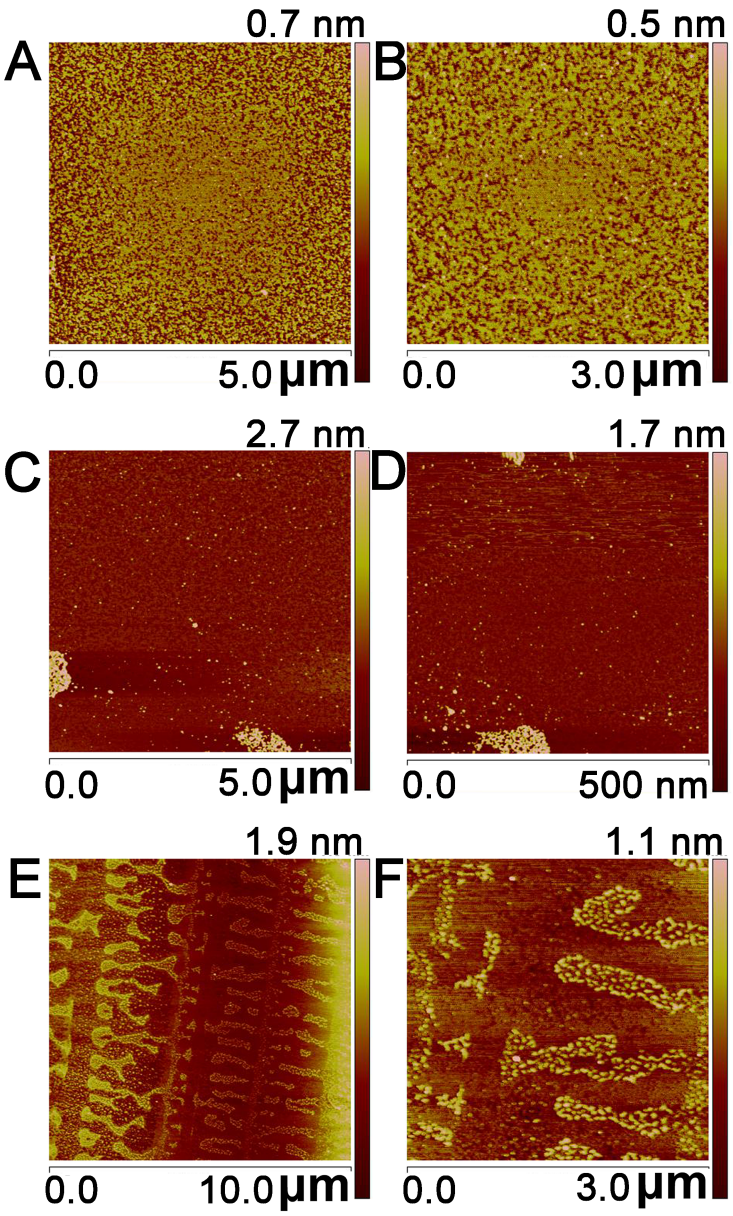

Figure S6. AFM images of Au NCs synthesized using LPA (A, B), DPA (C, D) and DLPA (E, F) as scaffolds.

For further characterizations of such dispersed small Au NCs, atomic force microscope (AFM) was utilized for the height determination of such Au NCs synthesized using chiral PA as scaffolds. As shown in Figure S6 A, there were large density of L-Au NCs on the surface of mica with the height range from 0.3 nm to 0.7 nm in a 5.0 μm × 5.0 μm area. The AFM images indicated the diameters of L-Au NCs were so small that the Au NCs with a diameter of about 1.5 nm in Figure 1A and Figure 1B might be the aggregations of real small Au NCs. To get a higher resolution AFM image of L-Au NCs, Au NCs with LPA as scaffolds were observed in a 3.0 μm × 3.0 μm area as shown in Figure S6 B. The AFM images of D-Au NCs and DL-Au NCs were similar to those of L-Au NCs which were shown from Figure S6 C to Figure S6 F. As shown in Figure S6 C and Figure S6 D, the heights of Au NCs with DPA as scaffold were about 1.5 nm which were consistent with the TEM images of D-Au NCs shown in Figure 1C and Figure 1D. Similarly, the AFM images of DL-Au NCs indicated that the heights of Au NCs with DLPA as scaffolds were about 1.0 nm which were coincident with the TEM images of DL-Au NCs shown in Figure 1E and Figure 1F. Overall, the AFM characterizations confirmed the formations of Au NCs synthesized using chiral PA as scaffolds and the good dispersion of such synthesized Au NCs in double-distilled water.

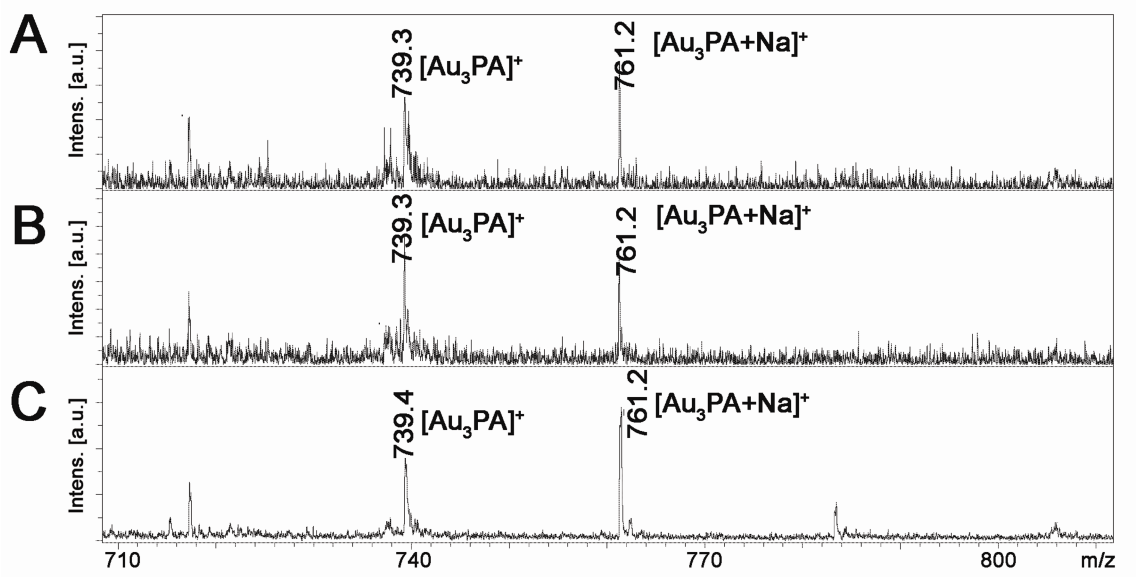

Figure S7. MALDI-TOF/TOF mass spectra of the Au NCs protected with different scaffolds such as LPA (A), DPA (B) and DLPA (C).

To determine what were the actually structures of the Au NCs protected by chiral PA and how many gold atoms formed the Au NCs, MALDI-TOF/TOF-MS was utilized for the characterizations of the Au NCs. The MALDI-TOF/TOF mass spectra of chiral PA protected Au NCs showed that the present Au NCs contained a small number of gold atoms such as Au_3. As shown in Figure S7 A, the peaks at 739.3 and 761.2 could be assigned to be the species $[Au_3PA]^+$ and $[Au_3PANa]^+$, respectively, which meant that such synthesized Au NCs mostly consisted of three Au atoms. However, these Au_3 clusters could easily aggregate to form larger Au NCs and the TEM and AFM images of these large Au NCs were shown in Figure 1 and Figure S6. As shown in Figure S7 B, D-Au NCs displayed similar MALDI-TOF/TOF-MS spectra to the spectra of L-Au NCs, most of the Au NCs with DPA as scaffolds were constructed with three Au atoms such as $[Au_3PA]^+$ and $[Au_3PANa]^+$. The MALDI-TOF/TOF spectra of DL-Au NCs showed very similar results from those of L-Au NCs and D-Au NCs. As shown in Figure S7 C, there were also two peaks at 739.3 and 761.2 which were corresponding to $[Au_3PA]^+$ and $[Au_3PANa]^+$ in the mass spectra of DL-Au NCs. In view of the MALDI-TOF/TOF spectra of the Au NCs, there were only Au_3 clusters and no other Au NCs which meant that Au_3 clusters were stable under such condition.

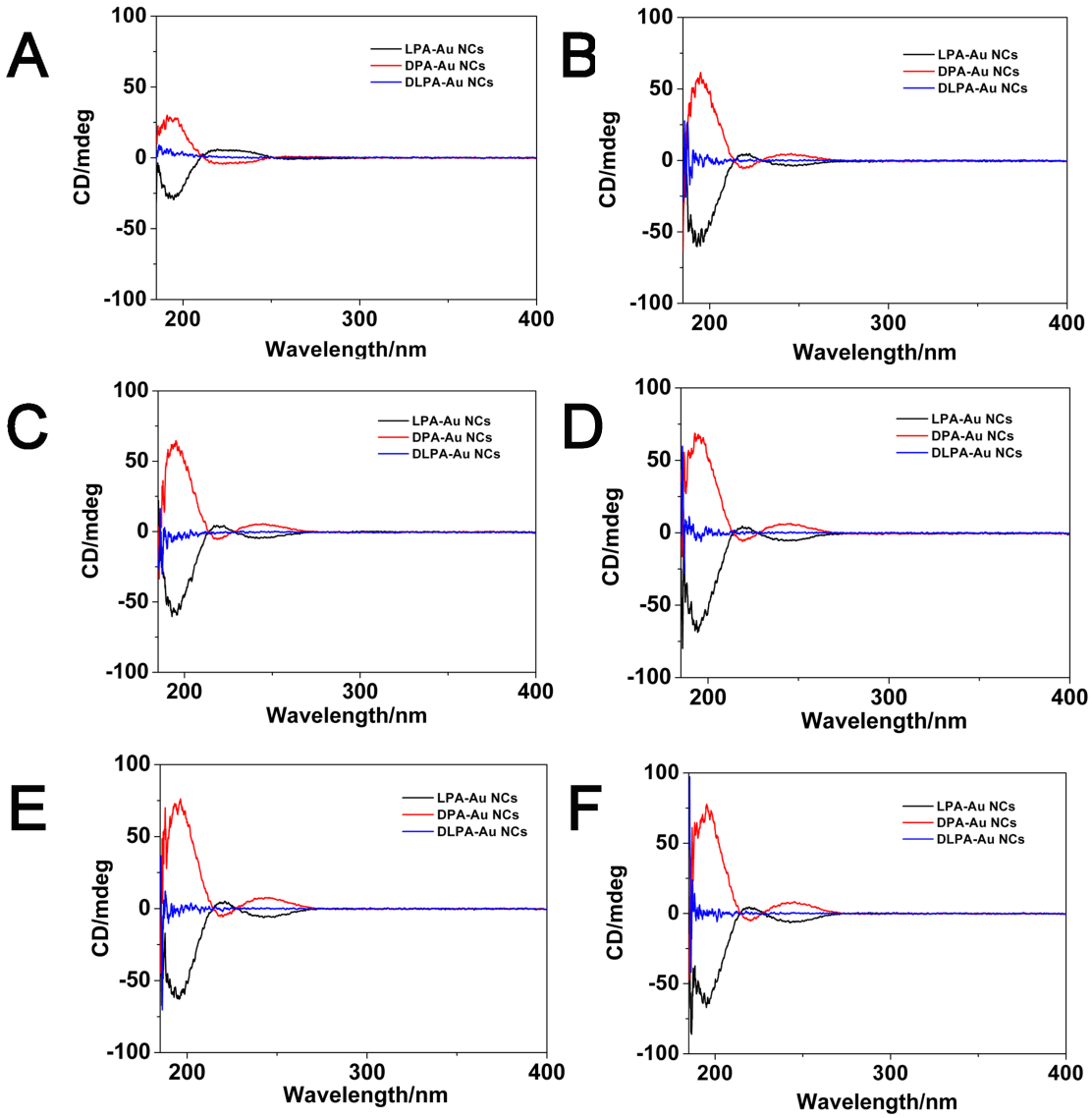

Figure S8. The investigation of in situ CD spectra of chiral PA protected Au NCs. The reaction time: A: 0 h, B: 0.5 h, C:2 h, D: 5 h, E: 10 h and D: 15 h.

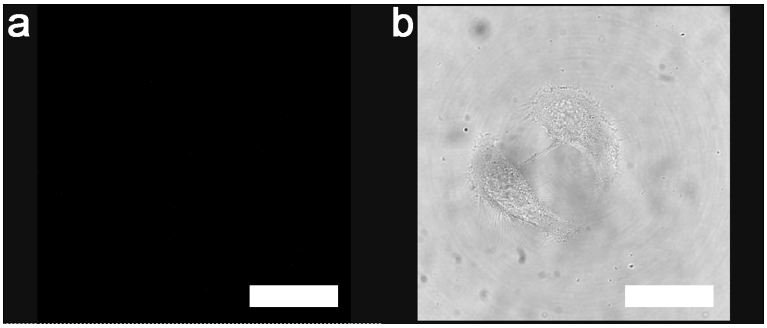

Figure S9. Confocal image of HeLa cells after incubation in cell culture fluid for 2 h, scale bars: 20 μm.

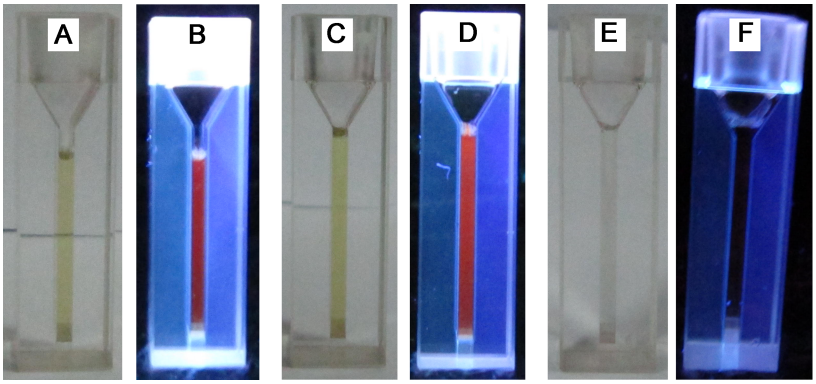

Figure S10. The photos of L-Au NCs (A), D-Au NCs (C) and DL-Au NCs (E) and the images of L-Au NCs (B), D-Au NCs (D) and DL-Au NCs (F) irradiation of UV light (365 nm).

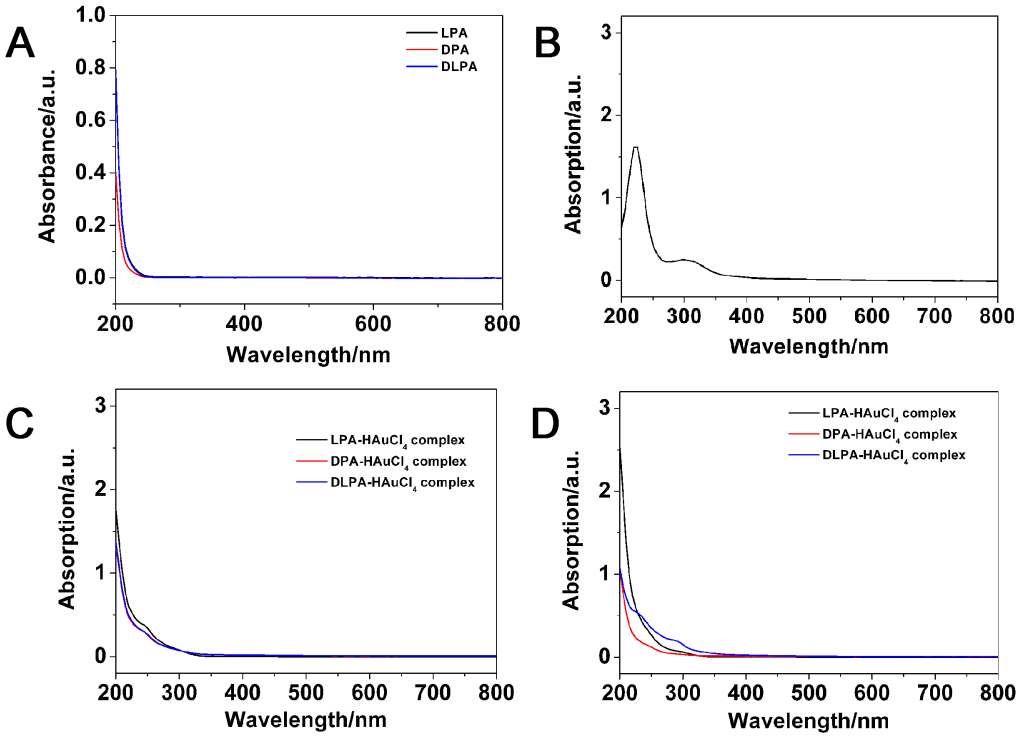

Figure S11. The UV-Vis absorption spectra of chiral PA (A), $HAuCl_4$ (B), the mixture of chiral PA and $HAuCl_4$ (C) and the mixture of chiral PA and $HAuCl_4$ after 15 h (D).

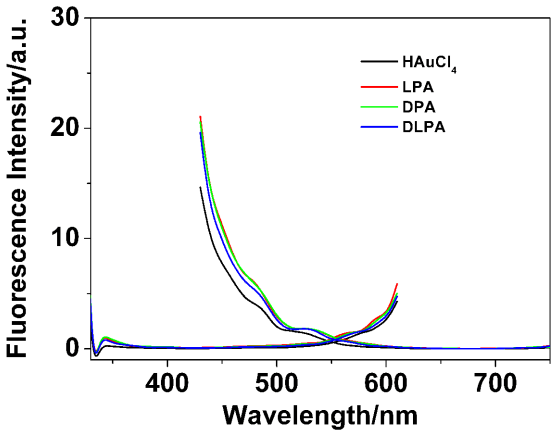

Figure S12. The photoluminescence spectra of $HAuCl_4$ and chiral PA.

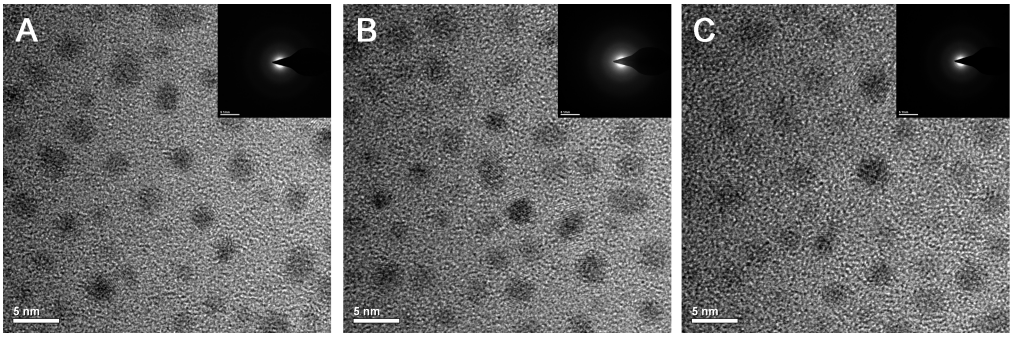

Figure S13. Typical TEM images of L-Au NCs (A), D-Au NCs (B) and DL-Au NCs (C) and the corresponding selected area electron diffraction pattern (inset).

As shown in Figure S13, there was no obvious symmetrical lattice in the selected area electron diffraction patterns which reflected that such synthesized chiral PA protected Au NCs were not so well crystalline.

The quantum yield (Q) of chiral PA protected Au NCs were calculated with the following equation. Quinine sulfate in 0.1 M H2SO4 (literature quantum yield 0.54 at 360 nm) was chose as a standard. Since Q is the quantum yield, I is the measured integrated emission intensity, n is the refractive index, and A is the optical density. The subscript R refers to the reference fluorophore of known quantum yield.

$$Q = Q_R \frac{I}{I_R} \frac{A_R}{A} \frac{n^2}{n_R^2} \quad [1]$$

Sample	Intergrated emission intensity (I)	Abs. At 360 nm (A)	Refractive index of solvent (n)	Quantum yield at 360 nm (Q)
Quinine sulfate	1119.37	0.1335	1.33	0.54 (known)
L-Au NCs	169.96	0.2004	1.33	0.01
D-Au NCs	31.12	0.2027	1.33	0.054
Ref. 2				0.003
Ref. 3				< 0.003
Ref. 4				0.007
Ref. 5				0.06

Table S1. The fluorescence quantum yield of chiral PA protected Au NCs and the comparisons with other Au NCs reported before.

Reference:

[1] Y. H. Yang, J. H. Cui, M. T. Zheng, C. F. Hu, S. Z. Tan, Y. Xiao, Q. Yang, Y. L. Liu, Chem. Commun. 2012, 48, 380-382.

[2] T. Huang, R. W. Murray, J. Phys. Chem. B 2001, 105, 12498-12502.

[3] Y. Y. Yang, S. W. Chen, Nano. Lett. 2003, 3, 72-79.

[4] Y. C. Negishi, Y. Takasugi, S. Sato, H. Yao, K. Kimura, T. Tsukuda, J. Am. Chem. Soc. 2004, 126, 6518-6519.

[5] J. P. Xie, Y. G. Zheng, J. Y. Ying, J. Am. Chem. Soc. 2009, 131, 888-889.